Journal of Computer-Aided Materials Design (2006) 13:111–129
DOI 10.1007/s10820-006-9019-8

Born–Oppenheimer interatomic forces from simple, local kinetic energy density functionals

V.V. KARASIEV[a,*], S.B. TRICKEY[b] and FRANK E. HARRIS[c]
[a] *Quantum Theory Project, Departments of Physics and of Chemistry, University of Florida, Gainesville, FL 32611, USA and Centro de Química, Instituto Venezolano de Investigaciones Científicas, IVIC, Apartado 21827, Caracas 1020-A, Venezuela*
[b] *Quantum Theory Project, Departments of Physics and of Chemistry, University of Florida, Gainesville, FL 32611, USA*
[c] *Department of Physics, University of Utah, Salt Lake City, UT and Quantum Theory Project, Departments of Physics and of Chemistry, University of Florida, Gainesville, FL 32611, USA*

Received 21 September 2005; Accepted 29 March 2006; Published online 25 July 2006

Abstract. Rapid calculation of Born–Oppenheimer (B–O) forces is essential for driving the so-called quantum region of a multi-scale molecular dynamics simulation. The success of density functional theory (DFT) with modern exchange-correlation approximations makes DFT an appealing choice for this role. But conventional Kohn–Sham DFT, even with various linear-scaling implementations, really is not fast enough to meet the challenge of complicated chemo-mechanical phenomena (e.g. stress-induced cracking in the presence of a solvent). Moreover, those schemes involve approximations that are difficult to check practically or to validate formally. A popular alternative, Car-Parrinello dynamics, does not guarantee motion on the B–O surface. Another approach, orbital-free DFT, is appealing but has proven difficult to implement because of the challenge of constructing reliable orbital-free (OF) approximations to the kinetic energy (KE) functional. To be maximally useful for multi-scale simulations, an OF-KE functional must be local (i.e. one-point). This requirement eliminates the two-point functionals designed to have proper linear-response behavior in the weakly inhomogeneous limit. In the face of these difficulties, we demonstrate that there is a way forward. By requiring *only* that the approximate functional deliver high-quality forces, by exploiting the "conjointness" hypothesis of Lee, Lee, and Parr, by enforcing a basic positivity constraint, and by parameterizing to a carefully selected, small set of molecules we are able to generate a KE functional that does a good job of describing various $H_q Si_m O_n$ clusters as well as CO (providing encouraging evidence of transferability). In addition to that positive result, we discuss several major negative results. First is definitive proof that the conjointness hypothesis is not correct, but nevertheless is useful. The second is the failure of a considerable variety of published KE functionals of the generalized gradient approximation type. Those functionals yield no minimum on the energy surface and give completely incorrect forces. In all cases, the problem can be traced to incorrect behavior of the functionals near the nuclei. Third, the seemingly obvious strategy of direct numerical fitting of OF-KE functional parameters to reproduce the energy surface of selected molecules is unsuccessful. The functionals that result are completely untransferable.

Keywords: conjointness, density functional theory, forces, orbital-free kinetic energy

1. Introduction

Incorporation of bonding and surface formation effects in a chemically realistic way is an essential ingredient for any simulation of chemo-mechanical processes. As noted in other places in this collection, our focus problem is tensile fracture of silica in

*To whom correspondence should be addressed. E-mail: vkarasev@qtp.ufl.edu

the presence of water. We adopt the contemporary multi-scale paradigm of nested zones. In the innermost zone, the immediate fracture region, the minimal acceptable quantum mechanical treatment is at the level of Born–Oppenheimer (B–O) forces as input to an otherwise classical molecular dynamics (MD) procedure. That zone conventionally is called, perhaps confusingly, the QM region. Forces between nuclei in the enclosing zone are calculated from classical potentials. Their compatibility with the QM forces is discussed elsewhere in this collection. This nested partitioning paradigm, called multi-scale simulation in the computational materials community, is called QM/MM methodology in the computational biology community.

Computing the B–O potential via density functional theory (DFT) [1–15] is a popular, promising route with well-advertised advantages and limitations. Because of the utility of the Kohn–Sham (KS) variational procedure [16], DFT as generally implemented involves more than strictly the electron number density. Operationally this means either the solution of a problem that scales asymptotically as N^3 at best, with N proportional to the total particle number, or pursuit of so-called order-N approximations, or acceptance of an approximate B–O mechanics via the Car-Parrinello method [17].

Orbital-free DFT (OF-DFT), i.e., a strictly density-parameterized theory without the KS equations, thus is an appealing potential alternative. But there are well-known obstacles to its implementation. In the next section, we give a brief review of those obstacles. There follows a summary of contemporary work with fairly complicated orbital-free Kinetic energy (OF-KE) density functionals. The following section gives a pedagogically motivated development of OF-KE density functionals based on the gradient expansion and the generalized gradient approximation. Then we consider constraints on OF-KE functionals and introduce the "conjointness" hypothesis. We then discuss functional forms already in the literature, some of which are of "conjoint" form and explore the deficiencies of the obvious strategy of fitting the parameters in those functionals so as to reproduce the B–O energy surfaces of selected molecules. This leads to a modification of the conjoint functional that is designed exclusively for the calculation of B–O forces in multi-scale MD simulations. For simplicity and speed, we require the functional to be local, applicable beyond the set of molecules used to determine its parameters, and capable of yielding accurate forces on the nuclei. By matching a critically important positivity constraint and parameterizing to a small set of carefully selected molecules, we achieve significant success. We illustrate with OF-KE functionals parameterized to the deformation of one, and of three Si–O bonds (in different molecules) and applied to more general deformations of several $H_qSi_mO_n$ clusters and to CO. Qualitatively correct, quantitatively reasonable forces are obtained for the clusters, and there is a reasonable degree of transferability to the less similar molecule CO.

2. Basics and historical barriers

Construction of an accurate approximation for the total KE, $T = \langle\Psi|\hat{T}|\Psi\rangle$, of a many-electron system in state $|\Psi\rangle$ as an explicit electronic density functional, $T = T[n_\Psi]$, is an important unresolved task in DFT. A review of previous work on KE functionals, with extensive references, is found in Ref. [18]. The KS procedure identifies the kinetic energy $T_s[n]$ of a model non-interacting Fermion system of the same density n, and evaluates that KE in terms of the KS orbitals:

$$T_s[\{\phi_i\}_{i=1}^N] = \sum_{i=1}^{N} \int \phi_i^*(\mathbf{r}) \left(-\frac{1}{2}\nabla^2\right) \phi_i(\mathbf{r}) d^3\mathbf{r} \equiv \int t_{\text{orb}}(\mathbf{r}) d^3\mathbf{r}. \tag{1}$$

(Hartree atomic units are used except where noted.) The remainder, $T - T_s$, is an ingredient of the exchange-correlation functional $E_{xc}[n]$.

There are at least two reasons to focus effort on OF approximations to $T_s[n]$ rather than $T[n]$. First, essentially all successful E_{xc} approximations assume the KS decomposition of the KE. Second, the underlying definition of T_s is via constrained-search [19]:

$$T_s[n] = \min_{\psi \mapsto n} \langle \psi | \hat{T} | \psi \rangle \,. \tag{2}$$

Immediately $T[n] \geq T_s[n]$. By density scaling arguments [20], it follows that $T_s[n]$ is the best possible lower bound to $T[n]$.

Given a $T_s[n]$ expression, the total system energy (electronic plus inter-nuclear repulsion) could be expressed as an orbital-free density functional

$$E^{\text{OF-DFT}}[n] = T_s[n] + E_{ne}[n] + E_H[n] + E_{xc}[n] + E_{\text{ion}} \tag{3}$$

with $E_{ne}[n]$, $E_H[n]$, $E_{xc}[n]$, and E_{ion} the usual nuclear-electron attraction, Hartree (or classical Coulomb) electron repulsion, electron exchange-correlation functionals, and nuclear-nuclear repulsion (or ion–ion repulsion in the case of pseudopotentials), respectively. For multi-scale simulations the appeal of Eq. (3) is virtually self-evident. The B–O force on nucleus I is simply the negative of the gradient with respect to the nuclear position $\mathbf{R}_I$ of $E^{\text{OF-DFT}}[n]$, so

$$\begin{aligned} \mathbf{F}_I &\equiv -\nabla_{\mathbf{R}_I} E^{\text{OF-DFT}}[n] \\ &= -\nabla_{\mathbf{R}_I} E_{\text{ion}} - \int \frac{\partial v_{\text{ext}}(\mathbf{r})}{\partial \mathbf{R}_I} n(\mathbf{r})\, d^3\mathbf{r} - \int \left[\frac{\delta T_s[n]}{\delta n(\mathbf{r})} + v_{\text{KS}}([n]; \mathbf{r}) \right] \frac{\partial n(\mathbf{r})}{\partial \mathbf{R}_I}\, d^3\mathbf{r}, \end{aligned} \tag{4}$$

where v_{ext} is the external potential (of the nuclei or ions) and v_{KS} is the effective potential corresponding to the sum of the functional derivatives (with respect to density) of the second through fourth terms of Eq. (3). Moreover, instead of a KS self-consistent field problem for N KS orbitals, the variational minimization yields a single "hydrodynamic" Euler equation:

$$\frac{\delta T_s[n]}{\delta n(\mathbf{r})} + v_{\text{KS}}([n]; \mathbf{r}) = \mu \,. \tag{5}$$

Here μ is the Lagrange multiplier that enforces density normalization, $\int n(\mathbf{r}) d\mathbf{r} = N$. In terms of the density obtained as the solution of Eq. (5), the B–O force, Eq. (4), reduces to

$$\mathbf{F}_I = -\nabla_{\mathbf{R}_I} E_{\text{ion}} - \int \frac{\partial v_{\text{ext}}(\mathbf{r})}{\partial \mathbf{R}_I} n(\mathbf{r})\, d^3\mathbf{r} - \mu \int \frac{\partial n(\mathbf{r})}{\partial \mathbf{R}_I}\, d^3\mathbf{r} \,. \tag{6}$$

Ordinarily the simulation volume at any given step is fixed, hence the order of integration and differentiation in the last term of this equation can be interchanged to

give the gradient of the total electron number, which is zero. Thus the usual working version of Eq. (6) is

$$\mathbf{F}_I = -\nabla_{\mathbf{R}_I} E_{\text{ion}} - \int \frac{\partial v_{\text{ext}}(\mathbf{r})}{\partial \mathbf{R}_I} n(\mathbf{r})\, d^3\mathbf{r}. \tag{7}$$

Because the KE is an order of magnitude larger then E_{xc}, Eq. (4) shows that the biggest error in the calculated force arises from the gradient of the approximate $T_s[n]$ functional.

We are far, of course, from being the first workers to find an OF-DFT approach to simulations appealing. In fact, the earliest antecedent of DFT was OF, namely the venerable Thomas–Fermi (T–F) model [21–23]. The T–F theory illustrates both the appeal and the elusiveness of a realistic OF-DFT. Specifically, Teller's non-binding theorem [24] shows that the T–F model does not include molecular species. This is hardly promising for multi-scale simulation of bond breaking! But all is not bleak. The parameterized Thomas–Fermi–von Weizsäcker (TFW) [25] model

$$\begin{aligned} T_{\text{TFW}}[n] &= T_{\text{TF}}[n] + \lambda T_W[n] \\ T_{\text{TF}}[n] &= c_0 \int n^{5/3}(\mathbf{r}) d\mathbf{r} \\ T_{\text{W}}[n] &= \frac{1}{8} \int \frac{|\nabla n(\mathbf{r})|^2}{n(\mathbf{r})} d\mathbf{r} \end{aligned} \tag{8}$$

(with λ a parameter $0 \le \lambda \le 1$) when combined with $E_{ne}[n] + E_{ee}[n] + E_{xc}[n]$, does give a model that binds neutral systems and negative ions [23]. While the results are qualitatively correct in that sense, they are nowhere nearly realistic enough for our agenda. For use in what follows, the value of the constant c_0 in Eq. (8) makes T_{TF} exact for the homogeneous electron gas: $c_0 = \frac{3}{10}(3\pi^2)^{2/3}$. Conversely, T_{W} is a form appropriate to the strongly inhomogeneous limit.

3. Two-point functionals

For several years, Carter and co-workers have been strong proponents of OF-KE functionals for materials simulations. A helpful review of their work is Ref. [26]. To move beyond the limits of TFW theory, they adopt a strategy of focusing on the physical reality of the density that an OF-KE approximate functional generates. The strategy dates to Wang and Teter [27] and can be traced all the way back to the original Hohenberg–Kohn DFT paper [1]. Broadly speaking that strategy has been pursued by several others as well, notably Madden and co-workers [28] and Chacón and co-workers [29] and, more recently, Choly and Kaxiras [30]. To illustrate the main points, we sketch the argument advanced in the Wang–Carter review article just cited.

Their criterion for accuracy is the density-potential linear response function $\chi(\mathbf{r} - \mathbf{r}')$ generated by the candidate functional. This criterion arises from requiring that the approximate functionals generate realistic atomic and molecular electronic shell structure and corresponding Friedel oscillations in solids. Carter et al. identify correct linear response as being key to generating such density oscillations. In slightly

sloppy notation for Fourier transforms, a sketch of their approach is as follows. The real- and reciprocal-space density-potential response are

$$\begin{aligned}\delta n(\mathbf{r}) &= \int d\mathbf{r}'\chi(\mathbf{r}-\mathbf{r}')\delta v_{\mathrm{KS}}(\mathbf{r}') \\ \delta n(\mathbf{q}) &= \chi(\mathbf{q})\delta v_{\mathrm{KS}}(\mathbf{q}),\end{aligned} \tag{9}$$

where v_{KS} is the total KS potential. A chain-rule manipulation

$$\delta(\mathbf{r}-\mathbf{r}') = \int d\mathbf{r}'' \frac{\delta n(\mathbf{r})}{\delta v_{\mathrm{KS}}(\mathbf{r}'')}\frac{\delta v_{\mathrm{KS}}(\mathbf{r}'')}{\delta n(\mathbf{r}')}$$

and the variational minimum condition combine to give

$$\delta(\mathbf{q}-\mathbf{q}') = \chi(\mathbf{q})\frac{\delta v_{\mathrm{KS}}}{\delta n}(\mathbf{q},\mathbf{q}') = -\chi(\mathbf{q})\frac{\delta^2 T_S}{\delta n \delta n}(\mathbf{q},\mathbf{q}'), \tag{10}$$

where $\chi(\mathbf{q})$ is known in the weakly inhomogeneous limit; it is the Lindhard function.

Because Carter and co-workers start from the physics contained in a direct-space two-point object, $\chi(\mathbf{r}-\mathbf{r}')$, it is, perhaps, unsurprising that their approach leads to emphasis on various non-local density approximations. Again see Ref. [26]. Wang recently has made what appears to be significant progress relative to those results [31]. However another recent result is the proof by Blanc and Cancès [32] that the so-called "density-independent" version of these two-point functionals is unstable. Specifically, for relatively modest electron densities in an inhomogeneous system subject to periodic boundary conditions, the use of such OF-KE functionals in Eq. (3) gives an energy that is unbounded below. One might argue that this is unsurprising, since these two-point OF-KE models are calibrated to correct linear-response in the limit of the weakly inhomeogeneous electron gas. But that argument is not as obvious as it might seem at first blush when one considers the immense success of E_{xc} from the homogeneous electron gas, namely the LDA.

Irrespective of these difficulties, there is a pragmatic obstacle to following the response-function calibration route. Non-locality is a computationally burdensome complication. For optimum utility in multi-scale MD, the approximate OF-KE functionals should be local (i.e. one-point). Clearly, this locality requirement makes our task harder.

4. Gradient expansion functionals

Hodges [33] introduced a gradient expansion for $T_s[n]$,

$$T_s[n] = T_0[n] + T_2[n] + \text{higher order terms}, \tag{11}$$

where $T_0[n] = T_{\mathrm{TF}}[n]$ and $T_2[n] = \frac{1}{9}T_W[n]$. The second-order gradient approximation (SGA) to $T_s[n]$ corresponds to dropping the higher-order terms in Eq. (11):

$$T_s^{\mathrm{SGA}}[n] = T_0[n] + T_2[n]. \tag{12}$$

A related class of KE functionals can be written in the form of the generalized gradient approximation (GGA) [34] that has been highly successful in E_{xc} models:

$$T_s^{\mathrm{GGA}}[n] = c_0 \int n^{5/3}(\mathbf{r}) F_t(s(\mathbf{r}))d^3\mathbf{r}. \tag{13}$$

Here F_t is called the "enhancement factor" and the reduced density gradient is $s \equiv |\nabla n|/(2nk_F)$, with $k_F = (3\pi^2 n)^{1/3}$.

A more productive form for our purposes is to write $T_s[n]$ as the Weizsäcker energy T_{W}, plus a remainder, T_θ, known as the Pauli term (see, e.g. Refs. [35–37]):

$$T_s[n] = T_{\mathrm{W}}[n] + T_\theta[n]. \tag{14}$$

T_θ, which has been shown to be non-negative, has an exact expression in terms of KS orbitals. One can write

$$T_\theta[n] \equiv \int t_\theta([n];\mathbf{r}) d^3\mathbf{r}, \tag{15}$$

where t_θ is positive for all $\mathbf{r}$ [37]. Then it follows that

$$\begin{aligned} t_\theta([n];\mathbf{r}) &\equiv t_{\mathrm{orb}}(\mathbf{r}) - \sqrt{n(\mathbf{r})}\left(-\frac{1}{2}\nabla^2\right)\sqrt{n(\mathbf{r})} \\ &= t_{\mathrm{orb}}(\mathbf{r}) - t_W([n];\mathbf{r}) + \frac{1}{4}\nabla^2 n(\mathbf{r}) \geq 0. \end{aligned} \tag{16}$$

Here $t_W([n];\mathbf{r}) = |\nabla n(\mathbf{r})|^2/8n(\mathbf{r})$ t_{orb} was defined in Eq. (1), and, consistently with Eq. (8),

$$T_{\mathrm{W}}[n] = \int t_W([n],\mathbf{r})\, d\mathbf{r}. \tag{17}$$

If we write T_W in a form parallel with that of the GGA in Eq. (13),

$$T_{\mathrm{W}}[n] = c_0 \int n^{5/3}(\mathbf{r}) \frac{5}{3} s^2(\mathbf{r}) d^3\mathbf{r} \tag{18}$$

and introduce (see [18]) a modified enhancement factor $\tilde{F}_t$

$$\tilde{F}_t(s) = F_t(s) - \frac{5}{3}s^2 \tag{19}$$

the GGA KE functional can be written in the form

$$T_s^{\mathrm{GGA}}[n] = T_{\mathrm{W}}[n] + c_0 \int n^{5/3}(\mathbf{r}) \tilde{F}_t(s(\mathbf{r})) d^3\mathbf{r}. \tag{20}$$

The second term of Eq. (20) thus is an approximation to the Pauli term T_θ.

The kinetic energy in the local-scaling version of DFT has the same form as Eq. (14) (see Ref. [38]):

$$T_s[n] = T_{\mathrm{W}}[n] + \tfrac{1}{2}\int n^{5/3}(\mathbf{r}) A_N([n];\mathbf{r}) d^3\mathbf{r}, \tag{21}$$

where the modulating factor A_N is an implicit functional of the density. It is positive and can be expressed in terms of KS orbitals similarly to Eq. (16):

$$A_N([n];\mathbf{r}) = \frac{\sum_{i=1}^{N} \nabla\phi_i^*(\mathbf{r})\nabla\phi_i(\mathbf{r}) - \frac{1}{4}\frac{(\nabla n(\mathbf{r}))^2}{n(\mathbf{r})}}{n^{5/3}(\mathbf{r})}. \tag{22}$$

From Eqs. (14), (15), (20), and (21) we obtain a relationship, for the GGA approximation, among t_θ, A_N, and $\tilde{F}_t$:

$$t_\theta^{\mathrm{GGA}}([n];\mathbf{r}) = \frac{1}{2} n^{5/3}(\mathbf{r}) A_N^{\mathrm{GGA}}([n];\mathbf{r}) = c_0 n^{5/3}(\mathbf{r}) \tilde{F}_t(s(\mathbf{r})). \tag{23}$$

5. Constraints on the Behavior of OF-KE Approximations

A major sub-genre of the DFT literature is devoted to scaling and other constraints on approximate functionals. Because of the importance of E_{xc}, the majority of that work focuses on E_{xc}: scaling constraints have played a major role in improving non-empirical E_{xc} approximations. With that successful example, it is only reasonable to ask what constraints are important for T_s.

With T_{W} explicitly separated in the KE functional as in Eq. (14), the Euler equation, Eq. (5), can be brought to Schrödinger-like form, to wit

$$\left(-\frac{1}{2}\nabla^2 + v_\theta([n];\mathbf{r}) + v_{\mathrm{KS}}([n];\mathbf{r})\right)\sqrt{n(\mathbf{r})} = \mu\sqrt{n(\mathbf{r})}\,. \tag{24}$$

Here the "Pauli potential" is

$$v_\theta([n];\mathbf{r}) \equiv \delta T_\theta[n]/\delta n(\mathbf{r})\,. \tag{25}$$

It can be shown [37, 39, 40] that for all $\mathbf{r}$

$$v_\theta([n];\mathbf{r}) \geq 0\,. \tag{26}$$

As we discuss in detail below, a *central* result of our research is that enforcement of Eq. (26) upon any approximation for $v_\theta([n];\mathbf{r})$ is a *crucial requirement*.

In addition to requiring the positiveness of $v_\theta([n];\mathbf{r})$, we next consider a few other constraints that so far have proved relevant.

In the weakly-inhomogeneous case ($s \approx 0$), the approximate KE functional should recover the SGA, Eq. (12), hence, the enhancement factor F_t should have the expansion

$$F_t(s) \underset{s\to 0}{=} 1 + \frac{1}{9}\cdot\frac{5}{3}s^2 = 1 + \frac{5}{27}s^2\,. \tag{27}$$

Then Eq. (19) gives

$$\tilde{F}_t(s) \underset{s\to 0}{=} 1 - \frac{40}{27}s^2. \tag{28}$$

For rapidly varying density $s \to \infty$, the opposite asymptotic case, it is generally thought that the von Weizsäcker term is correct [4]. Therefore, some functionals incorporate that limit for F_t in the form

$$F_t(s) \underset{s\to\infty}{=} \frac{5}{3}s^2, \tag{29}$$

which is equivalent to

$$\tilde{F}_t(s) \underset{s\to\infty}{=} 0. \tag{30}$$

Both Eqs. (28) and (30) provide additional constraints on any approximate OF-KE functional. There are other constraints, some of which will be satisfied automatically by the type of functional form ("modified conjoint") we eventually adopt; see below. But it also is important to get rid of one supposed constraint that is not, in fact, correct. Gál and Nagy [41] claim to show that if T_s is a functional *only* of the density and its gradient, then T_s must have a "generalized Weizsäcker form" and, by implication therefore, so must T_θ. But their argument is based on a supposed homogeneity-of-degree-one relationship [42] that is known to be incorrect [20]. More recently Gál [43] attempted to validate the Gál–Nagy result via a functional that is homogeneous of degree one for any integer particle number but is not otherwise. It appears to us that his argument is also incorrect, since the Gál–Nagy criteria derive from an argument that must be true for *arbitrary* densities. Thus we have seen no reason to attempt to impose the Gál–Nagy constraints.

6. Conjointness

Several authors have explored the concept of "conjointness" that was conjectured by Lee, Lee, and Parr (LLP) [44] to construct kinetic energy functionals. Examples include Refs. [45–49]. The LLP conjointness conjecture is that KE functionals may be constructed in the form of Eq. (13) using the same analytical function for the enhancement factor $F_t(s)$ as the function $F_x(s)$ used in the GGA exchange energy functionals

$$E_x^{\mathrm{GGA}}[n] = -c_x \int n^{4/3}(\mathbf{r}) F_x(s(\mathbf{r})) d^3\mathbf{r}. \tag{31}$$

We have found this idea very suggestive but not correct in general. Details follow.

7. Comparison of existing local functionals

As a first step, we compare the behavior of six local KE functionals proposed by others. These are:

1. The PW91 KE functional constructed by Lacks and Gordon [45]. It depends upon conjointness in that it starts from the Perdew–Wang 91 exchange functional;
2. The Tran–Wesolowski functional [49] (PBE-TW), which includes an enhancement factor defined by a simple function first used for E_x by Becke [50] and later by Perdew et al. [51]:

$$F_t^{\text{PBE-TW}}(s) = 1 + \frac{C_1 s^2}{1 + a_1 s^2} \tag{32}$$

with $C_1 = 0.2319$ and $a_1 = 0.2748$. The two parameters in the PBE-TW functional were adjusted to reproduce exactly the KE of the He and Xe atoms. Because the enhancement factor is not precisely the same as in the underlying E_x approximation, the PBE-TW functional is not strictly a conjoint functional, but it is close enough to be considered such. It is claimed to be among the most accurate GGA KE functionals;

3. A GGA functional proposed by Perdew [34] (GGA-Perdew);
4. A functional due to DePristo and Kress (DPK) [52] constructed in the form of a Padé approximant and satisfying the limiting conditions of Eqs. (27) and (29);
5. A functional introduced by Thakkar [53] with parameters fitted to the KEs of 77 molecules. This functional also is claimed to be one of the most accurate functionals of the GGA form;
6. The SGA functional, Eq. (12).

We assessed the functionals by comparing their numerical results with the results of conventional KS calculations in the local density approximation (LDA), using standard methods as found in Refs. [54–61]. The reference KS calculations were done in a triple-zeta basis with polarization functions [62–64]. All integrals were calculated by numerical quadrature that follows Becke's use of weight functions localized near each center to represent the multicenter integrals exactly as a sum of (distorted) atomic integrals [65]. Radial integration of the resulting single-center forms was via a Gauss-Legendre procedure, while integration over the angular variables used high-order quadrature formulas developed by Lebedev and Laikov [66]. The actual routines were downloaded from Ref. [67]. These computations were performed using routines developed by Salvador and Mayer [68] and included in their code FUZZY. With the KS density for a particular system, we then evaluated the total energy $E^{\text{OF-DFT}}$ from Eq. (3) and the interatomic forces from Eq. (4) for each OF-KE functional under study.

Because of our focus on brittle fracture, our first assessment step for these functionals was to examine the B–O forces they predict for SiO as a function of bond length. Despite the fact that the conventional KS LDA E_{tot} curve gives a proper, stable SiO bond at a reasonable bond length, none of the six OF-KE functionals predicts an energy minimum. By implication, the forces from these OF-KE functionals and parameters will be completely incorrect in the important region at and beyond the equilibrium bond length, where attractive interatomic forces should dominate. This deficiency is shown clearly in Figure 1, which displays the gradients of the total energy. We have therefore a key finding: with published parameters and a correct KS density as input, none of the approximate functionals predicts stability for this molecule.

A first step in analysis of this behavior is to rewrite these KE functionals in forms that expose their enhancement factors F_t and $\tilde{F}_t$ (either implicit or explicit) for the small and large-s limits. Table 1 shows that none of the approximate functionals behaves strictly properly at $s = \infty$, though DPK is off only by a constant; compare Eqs. (29) and (30). But this asymptote is of little importance in real materials and molecules, so it is doubtful that this misbehavior is the source of such bad results. In particular, we note that all the approximate KE functionals, except Thakkar's, have formally correct or almost correct behavior at small s as defined by Eq. (27) for F_t and Eq. (28) for $\tilde{F}_t$.

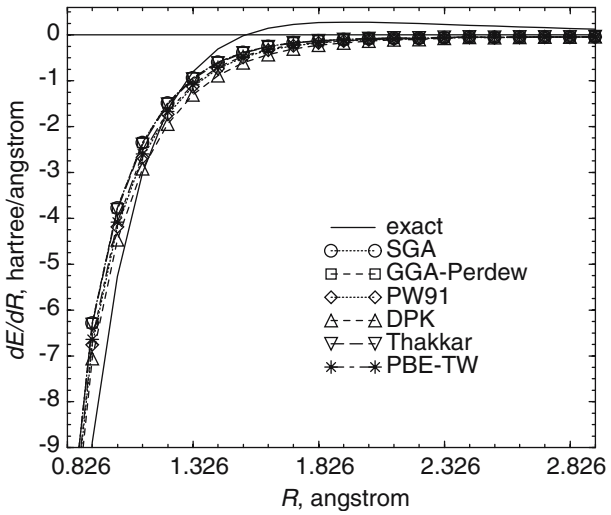

Figure 1. Gradients of the total energy of the SiO molecule as a function of the bond length, based on the LDA for E_{xc} and using the six OF-KE functionals described in Section 7. The "Exact" energy corresponds to T_s calculated directly from the KS orbitals in the conventional way; recall Eq. (1).

Table 1. Limiting behavior of F_t and $\tilde{F}_t$ enhancement factors as a function of the reduced density gradient s defined just after Eq. (13). All the data except for line are for the existing OF-KE functionals discussed in Section 7; PBE2 is a functional we have proposed

Functional	F_t as $s\to 0$	F_t as $s\to\infty$	$\tilde{F}_t$ as $s\to 0$	$\tilde{F}_t$ as $s\to\infty$
SGA	$1+0.1852s^2$	$0.1852s^2+1$	$1-1.4815s^2$	$-1.4815s^2+1$
GGA-Perdew	$1+0.1852s^2+O(s^4)$	$0.1856s^2+1+O(1/s^2)$	$1-1.4815s^2+O(s^4)$	$-1.4811s^2+1+O(1/s^2)$
PW91	$1+0.1235s^2+O(s^4)$	$O(1/s^2)$	$1-1.5432s^2+O(s^4)$	$-1.6667s^2+O(1/s^2)$
DPK	$1+0.1852s^2+O(s^4)$	$1.6667s^2-37.0035+O(1/s^2)$	$1-1.4815s^2+O(s^4)$	$-37.0035+O(1/s^2)$
Thakkar	$1-0.5613s\ +O(s^2)$	$O(s/\ln(s))$	$1-0.5613s\ +O(s^2)$	$-1.6667s^2+O(s/\ln(s))$
PBE-TW	$1+0.2319s^2+O(s^4)$	$1.8438+O(1/s^2)$	$1-1.4348s^2+O(s^4)$	$-1.6667s^2+1.8438+O(1/s^2)$
PBE2	$1+2.0309s^2+O(s^4)$	$7.9020+O(1/s^2)$	$1+0.3642s^2+O(s^4)$	$-1.6667s^2+7.9020+O(1/s^2)$

In fact, the KE of finite molecular systems is almost totally determined by the behavior of $\tilde{F}_t$ over a relatively small range of s, not the asymptotic regions. For example, in SiO at $R=1.926$ Å, the range $0.25\le s\le 1.25$ accounts for 99.7% of the total value of the PBE-TW functional. Therefore, in Figure 2 we show the various enhancement factors $\tilde{F}_t$ as functions of s^2 on the interval $[0,2]$. We did not expect to find that the SGA, GGA-Perdew, PW91, DPK, Thakkar, and PBE-TW enhancement factors (shown by the same long-dashed line) are indistinguishable on the scale of the figure for $s^2<1$. Their functional form over this entire range is quite close to that of the SGA: $\tilde{F}_t(s)=1-(40/27)s^2$.

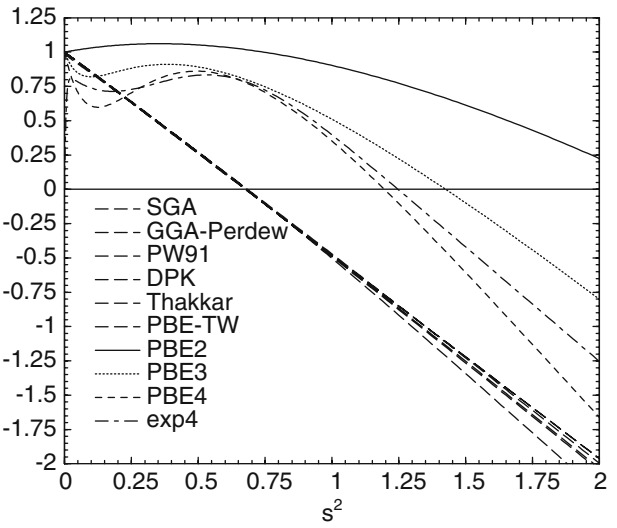

Figure 2. Enhancement factors $\tilde{F}_t$ of kinetic energy functionals as functions of s^2, where s is the reduced density gradient defined just after Eq. (13). The first six functionals in the legend are those previously proposed and discussed in Section 7; the remaining four are proposed in the present work.

For SiO at internuclear separation $R = 1.926\,\text{Å}$, the s values at the Si and O nuclei are 0.376 and 0.383, respectively, i.e. $s^2 \approx 0.14\ldots$ (Virtually the same values occur for the isolated Si and O atoms.) Inspection of Figure 2 shows that for this value of s^2 *all* the approximate functionals have $\tilde{F}_t$ values that are of the small-s form, rather close to $\tilde{F}_t = 1 - 1.5s^2$, or $\tilde{F}_t \approx 0.8$. In contrast, exact calculations of the modulating factor A_N for selected atoms [18, 69] show that $A_N([n]; \mathbf{r}) \to 0$ as $r \to 0$. This means that the Weizsäcker term gives a correct description of the kinetic energy density in the region close to the nucleus, equivalent to the statement that an optimum value of $\tilde{F}_t$ at the nucleus should be close to zero.

The poor behavior of $\tilde{F}_t$ near the nuclei has important consequences for the forces it generates. This fact follows by first rewriting Eq. (4) as

$$\mathbf{F}_I = -\nabla_{\mathbf{R}_I} E_{\text{ion}} - \int \frac{\partial v_{\text{ext}}(\mathbf{r})}{\partial \mathbf{R}_I} n(\mathbf{r})\, d^3\mathbf{r} - \int \left(\frac{\delta T_W[n]}{\delta n(\mathbf{r})} + v_\theta([n]; \mathbf{r}) + v_{\text{KS}}([n]; \mathbf{r}) \right) \frac{\partial n(\mathbf{r})}{\partial \mathbf{R}_I} d\mathbf{r}\,. \tag{33}$$

Thus, errors in the computed $\mathbf{F}_I$ arise from the replacement of the exact v_θ by its GGA approximation involving $\tilde{F}_t$. Next, from Eq. (23) combined with the definition of v_θ, it follows [70] that

$$v_\theta^{\text{GGA}}(\mathbf{r}) = \frac{5}{3} c_0 n^{2/3}(\mathbf{r}) \tilde{F}_t(s(\mathbf{r})) + c_0 n^{5/3}(\mathbf{r}) \frac{\partial \tilde{F}_t(s)}{\partial s} \times \left(\frac{\partial s(\mathbf{r})}{\partial n(\mathbf{r})} - \nabla \frac{\partial s(\mathbf{r})}{\partial \nabla n(\mathbf{r})} \right). \tag{34}$$

We may estimate v_θ^{GGA} near a nucleus ($r = 0$), where it is most important, from the nuclear-cusp behavior

$$n(\mathbf{r}) \sim \exp(-2Zr). \tag{35}$$

Taking $\tilde{F}_t(s) = 1 + as^2$, we find that

$$v_\theta^{\mathrm{GGA}}(r) \sim \frac{a}{r}, \tag{36}$$

which shows that the sign of v_θ^{GGA} is the same as that of a. Since $a < 0$ for all six published functionals, it follows that near the nuclei $v_\theta^{\mathrm{GGA}} < 0$, which is wrong: v_θ must be non-negative for all $\mathbf{r}$. The fact that v_θ^{GGA} is of the wrong sign in the most important part of its range inevitably leads to qualitatively incorrect force computations. It also means that the conjointness hypothesis cannot be strictly correct, another key result.

8. Modified conjoint KE functionals

Conjointness turns out to be useful nevertheless, as we shall show shortly. First, however, the central role of the total energy in QM makes it almost a reflex to attempt an OF-KE parameterization by searching for fits to total energies from direct KS computations. We considered, therefore, an exchange energy enhancement factor of the PBE form, given in Eq. (32). Its parameters were optimized for the molecule SiO by minimizing the error function

$$\omega_E = \sum_{i=1}^{m} |E_i^{\mathrm{KS}} - E_i^{\mathrm{OF\text{-}DFT}}|^2, \tag{37}$$

where i indexes particular nuclear configurations used for the fit and $E_i^{\mathrm{OF\text{-}DFT}}$ was evaluated using the KS density for that configuration.

This parameterization scheme failed. If the SiO bond lengths of the fitting set were distributed uniformly over both the attractive and repulsive regions of the KS potential curve, the resulting parameter set did not produce a minimum in the OF-DFT potential. Restriction of the fitting set to the attractive region of the KS curve did give an OF-DFT minimum, but the full curve exhibited oscillations and other nonphysical properties. Attempts to use more complicated analytical forms for F_t (motivated by other exchange approximations) in combination with Eq. (37) also failed.

Since total-energy parameterization fails at least for these simple functional forms, we are compelled to refocus on the original objective: an OF-KE functional parameterization solely for reproducing the KS forces, irrespective of the resulting total energy. We proceeded by determining functional parameters through minimization of the error function

$$\omega_{\Delta E} = \sum_{M,i} \left| \Delta E_{M,i}^{\mathrm{KS}} - \Delta E_{M,i}^{\mathrm{OF\text{-}DFT}} \right|^2, \tag{38}$$

where for nuclear configuration i of molecule M, $\Delta E = E_{M,i} - E_{M,e}$, with $E_{M,e}$ the energy associated with the equilibrium nuclear configuration as predicted from KS computations. Clearly this error function is a finite difference approximation to the B–O forces. It optimizes only the shape of the computed potential surface and is totally indifferent as to any uniform energy displacement from the KS surface.

We applied this parameterization scheme with two different training sets of molecules: (1) a single SiO diatomic, and (2) a three-molecule set consisting of SiO,

H_4SiO_4, and $H_6Si_2O_7$, but with nuclear configurations restricted to those reached by a single bond stretch (for H_4SiO_4 one of the Si–O bonds, for $H_6Si_2O_7$ one of the central Si–O bonds). It proved sufficient to use between 5 and 10 bond lengths distributed over the range $[R_e/2, 2R_e]$, where R_e is the equilibrium bond length as predicted by the KS-LDA calculations. Functionals found by using the form given in Eq. (32), but with parameter sets determined as described here, are designated PBE2.

In addition to the parametric form of Eq. (32), we examined the three- and four-parameter exchange energy enhancement factors introduced by Adamo and Barone [71]

$$F_t^{\mathrm{PBE3}}(s) = 1 + \frac{C_1 s^2}{1 + a_1 s^2} + \frac{C_2 s^4}{(1 + a_1 s^2)^2}$$
$$F_t^{\mathrm{PBE4}}(s) = 1 + \sum_{i=1}^{3} C_i \Big[\frac{s^2}{1 + a_1 s^2}\Big]^i. \tag{39}$$

We also considered a form for F_t with somewhat different behavior at intermediate values of s:

$$F_t^{\mathrm{exp4}}(s) = C_1(1 - e^{-a_1 s^2}) + C_2(1 - e^{-a_2 s^4}). \tag{40}$$

Our emphasis was exploration of simple F_t forms suggested by conjointness and compatible with multi-scale MD simulations of complex systems. The choices should not be construed as optimal in any other sense than that.

The first test was parameterization of a PBE2 functional by minimization of $\omega_{\Delta E}$ for six SiO bond lengths $R_i = \{1.126, 1.326, 1.526, 1.826, 2.126, 2.726\}$Å ; for it the KS equilibrium bond length is $R_e = 1.526$ Å. The resulting parameter values are shown in Table 2. The behavior of the corresponding F_t and $\tilde{F}_t$ in the limits $s \to 0$ and $s \to \infty$ is presented in the last line of Table 1 (designated PBE2). Note that, in contrast to the PBE-TW functional (which has the same form but different parameters), the small-s quadratic term of $\tilde{F}_t$ for the PBE2 functional has the positive sign necessary to cause the potential v_θ to have its required positive value near the nuclei. It is because of this that we designate such a functional as "modified conjoint".

Figure 3 compares the PBE-TW potential and its modified conjoint counterpart, PBE2. Observe that while both potentials deviate maximally from zero near the nuclei (identified from the maxima in the electron density), it is precisely in that region that the two approximate potentials differ most drastically, with $v_\theta^{\mathrm{PBE\text{-}TW}}$ diverging toward $-\infty$ at the nuclear positions.

Table 2. Parameters of approximate OF-KE functionals fitted to energy differences. PBE2 is fitted to one molecule, the others to three; see text

Functional	C_1	a_1	C_2	a_2	C_3
PBE2	2.0309	0.2942	–	–	–
PBE3	−3.7425	4.1355	50.258	–	–
PBE4	−7.2333	1.7107	61.645	–	−93.683
exp4	0.8524	199.81	1.2264	4.3476	–

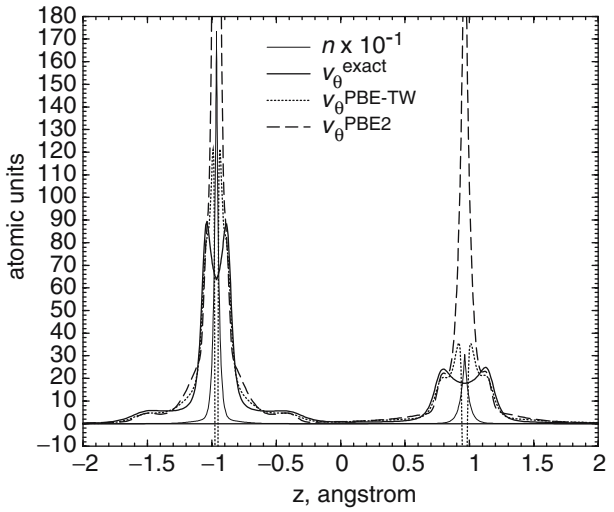

Figure 3. Two approximate kinetic energy functional derivatives $v_\theta = \delta T_\theta[n]/\delta n(\mathbf{r})$ corresponding to the PBE-TW kinetic energy functional and to the ΔE fit of the same functional form (PBE2 functional) for the SiO molecule at the stretched bond length $R = 1.926$ Å, evaluated at points z along the internuclear axis on which the Si and O nuclei are close to -1 and $+1$ angstrom respectively. For comparison we also show the electron density and the "exact" v_θ that results from conventional KS computations.

In Section 7, we showed that GGA KE functionals in general have values of v_θ that are singular at the nuclei; v_θ^{PBE2} is consistent with that. At least, $v_\theta^{\mathrm{PBE2}} \geq 0$ for all $\mathbf{r}$, with the result that it gives qualitatively reasonable forces. The exact v_θ is not only positive everywhere but also finite at the nuclei, so it is not surprising that the PBE2 functional overestimates the kinetic energy. Insight can be gained from the virial relation [37]

$$T_\theta[n] = \frac{1}{2}\int v_\theta([n];\mathbf{r})(3+\mathbf{r}\cdot\nabla)n(\mathbf{r})d^3\mathbf{r}. \tag{41}$$

For a more thorough exploration, we treated the three-molecule training set. For SiO, we used the six bond lengths listed earlier in this section, for H_4SiO_4 we fixed three Si–O bonds at the KS $R_e = 1.637$Å and varied the remaining Si–O bond over the set $R_i = \{1.237, 1.437, 1.637, 1.937, 2.237, 2.837\}$Å. For $H_6Si_2O_7$, the corresponding procedure was to hold one of the central Si–O bonds at the KS equilibrium value $R_e = 1.61$ Å and vary the other over the set $R_i = \{1.21, 1.41, 1.61, 1.91, 2.21, 2.81\}$ Å. Table 2 shows parameters for all the conjoint forms listed above (except PBE2) as obtained from minimization of $\omega_{\Delta E}$ over this training set.

The accuracy with which the forces are fitted for one of the molecules is shown in Figure 4. All the functionals describe the attractive region quite accurately while giving rather good results for the lower-energy part of the repulsive region. Only at R values shorter than about $R_e - 0.25$ Å are there major differences either among the approximate functionals or between them and the exact KS forces.

A more severe test of the new parameterizations is their ability to yield forces on molecules to which they were not fitted explicitly. A simple set of convenient cases involves bond deformations of the training-set molecules that were not used in the fit-

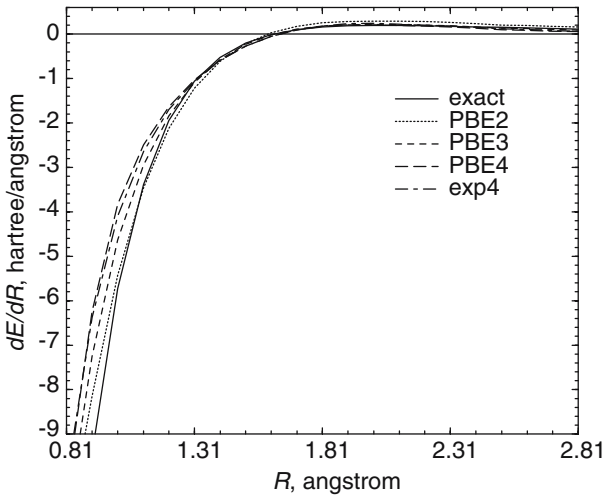

Figure 4. Exact and approximate values of dE/dR for the deformation of one of the central Si–O bonds in $H_6Si_2O_7$, calculated from fitted OF-KE functionals. "Exact" values are those given by conventional KS computation for the same E_{xc} approximation.

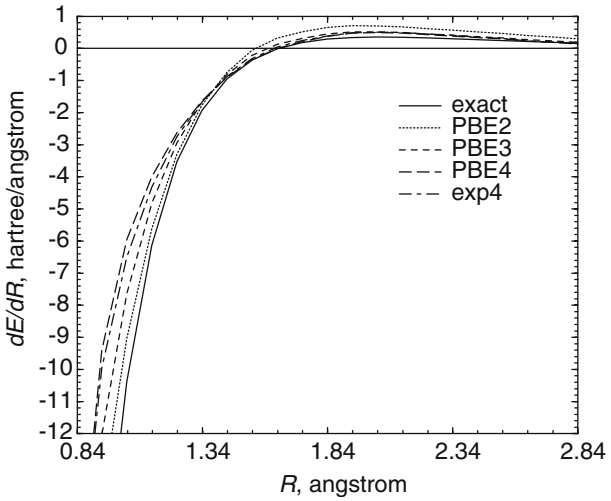

Figure 5. "Exact" KS and fitted OF-KE functional values of dE/dR for H_4SiO_4, with R the length of two of the four Si–O bonds; the other two Si–O bonds are kept at the equilibrium value. "Exact" values are those given by conventional KS computation for the same E_{xc} approximation.

ting. Figure 5 shows forces for the H_4SiO_4 molecule as two Si–O bonds are changed simultaneously by the same amount while the other two are held at R_e. Figure 6 is similar, but for the simultaneous change of three Si–O bonds with the fourth kept at R_e. All the new functionals except PBE2 predict the equilibrium distance (position where $\mathbf{F} = 0$) well. Moreover, except for PBE2, the forces are quite good in the attractive region and for short excursions into the repulsive region. We do note that the PBE2 functional becomes better than the other approximate functionals when far into the repulsive region. The other functionals diverge significantly from the exact curve in the region $R < 1.24\,\text{Å}$.

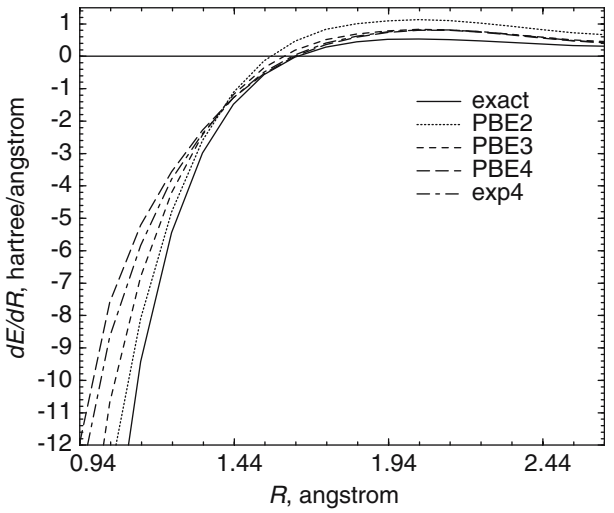

Figure 6. Values of dE/dR for SiO_4H_4, exact and calculated using fitted KE density functionals, where R is the length of three of the four Si–O bonds; the fourth Si–O bond is kept at the equilibrium value. "Exact" values are those given by conventional KS computation for the same E_{xc} approximation.

An even tougher test is the application of the new OF-KE functionals to a system outside the training set. We picked the CO diatomic molecule. The energy gradient predicted by each functional is shown in Figure 7. Given that the functionals had no information about carbon, there is a reasonable degree of transferability exhibited. In particular, the energy gradients in the longer-distance attractive region are very close to those from the reference KS calculation. However, the repulsive force is substantially too large, which results in a significant overestimate of the equilibrium bond length. Nevertheless, even for this relatively difficult test, a stable molecule is predicted by all the new approximate functionals.

Preliminary exploration of other training sets suggest that the parameters are to some extent sensitive to training set choice. At this stage of exploration we are unconcerned by that sensitivity, since we likely will follow a training strategy akin to that discussed by Mallik et al. in this collection.

9. Key findings

Our key findings are:

- The conjointness hypothesis per se is not valid;
- Conjointness is a useful, suggestive guide for initial construction of an OF-KE functional;
- It is *essential* to enforce (or at least achieve) positivity of v_θ;
- Parameterization to KS forces, not total energies, is key to making progress with a simple local OF-KE functional;
- A simple local OF-KE functional trained on one small set of molecules can give at least semi-quantitative results for an entirely different molecule

The explorations reported here suggest strongly that the combined use of the conjointness conjecture, v_θ positivity, and parameterization to forces alone is a promising route to an OF-KE functional useful in MD simulations. The next step is to

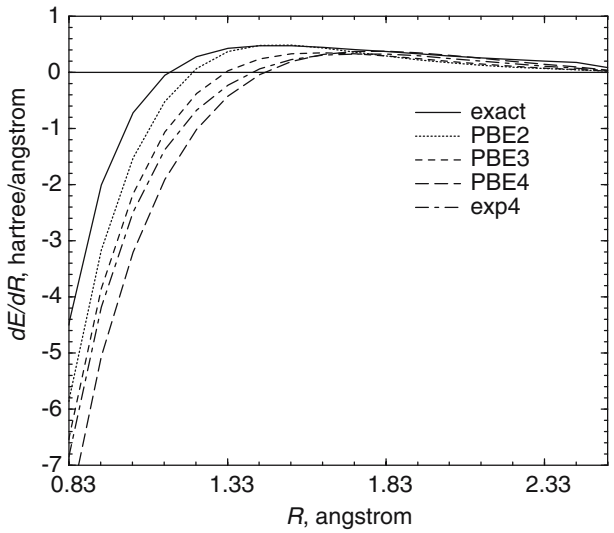

Figure 7. Exact and approximate gradients of the total energy for the CO molecule as a function of the bond length, calculated using fitted KE density functionals. "Exact" values are those given by conventional KS computation for the same E_{xc} approximation.

find computationally efficient refinements of the form of $\tilde{F}_t$ that will improve the fitted force curves. An obvious improvement is to eliminate the spurious singularity at the nuclei. Application of additional constraints (*e.g.* from uniform scaling) is another form of improvement that has seen great success in E_{xc} approximations and may be helpful for OF-KE approximations.

Once we have reasonable OF-KE functionals, a closely related task is to model the density $n(\mathbf{r})$ and its relaxation in response to nuclear motion, so that the model density works well with the approximate OF functional. We are exploring that issue.

Acknowledgments

This work was supported in part by the U.S. National Science Foundation, Grant DMR-0325553. FEH also acknowledges support from NSF grant PHY-0303412. SBT also acknowledges support from NSF grant DMR-0218957. VVK also acknowledges support from FONACIT of Venezuela through Group Project No. G-97000741.

References

1. Hohenberg, P. and Kohn, W., Phys. Rev. 136 (1964) B864–B871.
2. Jones, R.O. and Gunnarsson, O., Rev. Mod. Phys. 61 (1989) 689.
3. Parr, R.G. and Yang, W., Density Functional Theory of Atoms and Molecules, Oxford, NY, 1989.
4. Dreizler, R.M. and Gross, E.K.U., Density Functional Theory, Springer, Berlin, 1990.
5. Kryachko, E.S. and Ludeña, E.V., Energy Density Functional Theory of Many-Electron Systems, Kluwer, Dordrecht, 1990.
6. Trickey, S.B., (spec. ed.), Density Functional Theory for Many-Fermion Systems, Adv. Quant. Chem. 21, Academic, San Diego, 1990.
7. Gross, E.K.U. and Dreizler, R.M., (eds.) Density Functional Theory, Plenum, NY, 1995.

8. Seminario, J.M. and Politzer, P., (eds.), Modern Density Functional Theory, Elsevier, Amsterdam, 1995.
9. Chong, D.P., (ed.), Recent Advances in Density Functional Methods, World Scientific, Singapore, 1995.
10. Kohn, W., Becke, A.D. and Parr, R.G., J. Phys. Chem. 100 (1996) 12974.
11. Seminario, J.M. (ed.), Recent Developments and Applications of Modern Density Functional Theory, Elsevier, Amsterdam, 1996.
12. Nalewajski, R.F., (ed.), Density Functional Theory, Springer, Berlin, 1996.
13. Eschrig, H., The Fundamentals of Density Functional Theory, Teubner Texte für Physik 32, Teubner, Stuttgart and Leipzig, 1996.
14. Görling, A., Trickey, S.B., Gisdakis, P. and Rösch, N., in Topics in Organometallic Chemistry, vol. 4, P. Hoffmann, and J.M. Brown, eds. Springer, Berlin, 1999 109–63.
15. Koch, W. and Holthaussen, M.C., A Chemist's Guide to Density Functional Theory, Second Ed., Wiley VCH, Weinheim, 2001.
16. Kohn, W. and Sham, L.J., Phys. Rev. 140 (1965) A1133.
17. Car, R. and Parrinello, M., Phys. Rev. Lett. 55 (1985) 2471.
18. Ludeña, E.V. and Karasiev, V.V., in Reviews of Modern Quantum Chemistry: a Celebration of the Contributions of Robert Parr, edited by K. D. Sen, World Scientific, Singapore, 2002, p. 612.
19. Levy, M., Proc. Natl. Acad. Sci. USA 76 (1979) 6062.
20. Chan, G.K.-L. and Handy, N.C., Phys. Rev. A 59 (1999) 2670.
21. Thomas, L.H., Proc. Camb. Phil. Soc. 23 (1927) 542.
22. Fermi, E., Atti Accad. Nazl. Lincei 6 (1927) 602; Z. Phys. 48 (1928) 73.
23. Lieb, E.H., Rev. Mod. Phys. 53 (1981) 603.
24. Teller, E., Rev. Mod. Phys. 34 (1962) 627.
25. Von Weizsäcker, C.F., Z. Phys. 96 (1935) 431.
26. Wang, Y.A. and Carter, E.A., Orbital-free Kinetic-energy Density Functional Theory, Chap. 5 in Theoretical Methods in Condensed Phase Chemistry, edited by S.D. Schwartz, Kluwer, NY, 2000, p. 117 and references therein.
27. Wang, Y.A. and Teter, M.P., Phys. Rev. B 45 (1992) 13196.
28. Foley, M. and Madden, P.A., Phys. Rev. B 53 (1996) 10589 and refs. therein.
29. García-González, P., Alvarellos, J.E. and Chacòn, E., Phys. Rev. A 57 (1998) 4192 and refs. therein.
30. Choly, N. and Kaxiras, E., Sol. State. Commun. 121 (2002) 281.
31. Private communication, Wang, Y.A., to VVK and SBT, July, 2005, and to be published.
32. Blanc, X. and Cancès, E., J. Chem. Phys. 122 (2005) 214106.
33. Hodges, C.H., Can. J. Phys. 51 (1973) 1428.
34. Perdew, J.P., Phys. Lett. A 165 (1992) 79.
35. Tal, Y. and Bader, R.F.W., Int. J. Quantum Chem. S12 (1978) 153.
36. Bartolotti, L.J. and Acharya, P.K., J. Chem. Phys. 77 (1982) 4576.
37. Levy, M. and Ou-Yang, H., Phys. Rev. A 38 (1988) 625.
38. Ludeña, E.V., Karasiev, V., López-Boada, R., Valderrama, E. and Maldonado, J., J. Comp. Chem. 20 (1999) 155.
39. Levy, M., Perdew, J.P. and Sahni, V., Phys. Rev. A 30 (1984) 2745.
40. Herring, C., Phys. Rev. A 34 (1986) 2614.
41. Gál, T. and Nagy, A., J. Mol. Struct Theochem 501–502 (2000) 167.
42. Liu, S. and Parr, R.G., Chem. Phys. Lett. 278 (1997) 341.
43. Gál, T., Phys. Rev. A 64 (2001) 062503.
44. Lee, H., Lee, C. and Parr, R.G., Phys. Rev. A 44 (1991) 768.
45. Lacks, D.J. and Gordon, R.G., J. Chem. Phys. 100 (1994) 4446.
46. Lembarki, A. and Chermette, H., Phys. Rev. A 50 (1994) 5238.
47. Fuentealba, P. and Reyes, O., Chem. Phys. Lett. 232 (1995) 31.
48. Fuentealba, P., J. Mol. Struct. (THEOCHEM) 390 (1997) 1.
49. Tran, F. and Wesolowski, T.A., Int. J. Quantum Chem. 89 (2002) 441.
50. Becke, A.D., J. Chem. Phys. 84 (1986) 4524.
51. Perdew, J.P., Burke, K. and Ernzerhof, M., Phys. Rev. Lett. 77 (1996) 3865.

52. DePristo, A.E. and Kress, J.D., Phys. Rev. A 35 (1987) 438.
53. Thakkar, A.J., Phys. Rev. A 46 (1992) 6920.
54. Slater, J.C., Phys. Rev. 81 (1951) 385.
55. Slater, J.C., Phys. Rev. 82 (1951) 538.
56. Slater, J.C., J. Chem. Phys. 43 (1965) S228.
57. Gáspár, R., Acta Phys. Hung. 3 (1954) 263.
58. Kohn, W. and Sham, L.J., Phys. Rev. 140 (1965) A1133.
59. Tong, B.Y. and Sham, L.J., Phys. Rev. 144 (1966) 1.
60. Vosko, S.H., Wilk, L. and Nusair, M., Can. J. Phys. 58 (1980) 1200.
61. Ceperley, D.M. and Alder, B.J., Phys. Rev. Lett. 45 (1980) 566.
62. Schäfer, A., Horn, H. and Ahlrichs, R., J. Chem. Phys. 97 (1992) 2571.
63. Schäfer, A., Huber, C. and Ahlrichs, R., J. Chem. Phys. 100 (1994) 5829.
64. Taken from the Extensible Computational Chemistry Environment Basis Set Database, Version 02/25/04, Molecular Science Computing Facility, Environmental and Molecular Sciences Laboratory, Pacific Northwest Laboratory, P.O. Box 999, Richland, Washington 99352, USA, funded by the U.S. Department of Energy (contract DE-AC06-76RLO). See http://www.emsl.pnl.gov/forms/basisform.html
65. Becke, A.D., J. Chem. Phys. 88 (1988) 2547.
66. Lebedev, V.I. and Laikov, D.N., Dokl. Akad. Nauk 366 (1999) 741 [Dokl. Math. 59 (1999) 477].
67. Computational Chemistry List (CCL) Archives: http://www.ccl.net/
68. Salvador, P. and Mayer, I., J. Chem. Phys. 120 (2004) 5046.
69. Karasiev, V.V., Ludeña, E.V. and Artemyev, A.N., Phys. Rev. A 62 (2000) 062510.
70. Korn, G.A. and Korn, T.M., Mathematical Handbook for Scientists and Engineers, McGraw-Hill, NY, 1961.
71. Adamo, C. and Barone, V., J. Chem. Phys. 116 (2002) 5933.